Madencilik - Mining, 2024, 63(2), 86-94

BİLİMSEL MADENCİLİK DERGİSİ
SCIENTIFIC MINING JOURNAL

TMMOB Maden Mühendisleri Odası Yayını / The Publication of the Chamber of Mining Engineers of Turkey

www.mining.org.tr

Research Article

DEM aided investigation of the effects of screen surface properties on screening performance

Ahad Harzanak[a,*], E. Caner Orhan[b,**]

a Demir Export Inc., Research and Development Center, Ankara, TÜRKİYE
b Hacettepe University, Department of Mining Engineering, 06800, Beytepe, Ankara, TÜRKİYE

Received: 17 April 2024 • Accepted: 29 November 2024

A B S T R A C T

Under diverse conditions, multiple empirical models are employed to forecast screen performance. Although they provide good insight for the sizing and selection of screens, they generally are insufficient for the precise quantification of the effects of parameters such as surface dimensions, aperture shape/orientation, and surface open area. Discrete element modelling (DEM) has proved in many instances that it provides close-up examination of particle motion under various conditions for a variety of mineral processing operations and generates data that is not possible to obtain with conventional experimentation or sampling.

This study investigates the influence of screen surface parameters (i.e., surface dimensions, aperture orientation/shape and surface open area) on screening performance using the DEM method for the simulation of vibrating screens. To achieve realistic simulations, "multi-spheres" were used to represent particles with irregular shapes. The simulation results showed that particle motions were accurately predicted. Key findings include that longer screen surfaces increased screening efficiency and mass recovery in the undersize stream and screens with perpendicular apertures to the flow direction achieved higher screening efficiency. Additionally, increased surface open area improved screening efficiency by increasing the recovery of finer particles. These findings were evaluated using conventional screen efficiency criteria, and the separation of particles was also investigated in terms of size distribution of products and residence time of particles along the screen.

Keywords: *Discrete Element Method, Simulation, Vibrating Screen, LIGGGHTS Solver, Spherical Particles, Irregularly Shaped Particles.*

Introduction

Screening finds extensive application in various fields, including ore preparation and industries such as textiles, food, and recycling (Jeanger et al., 2022; Beas et al., 2021). In mineral processing applications, the dimensions, design, and performance of screens determine the efficiency and utilization of subsequent operations/processes. As a critical stage in these industries, optimizing screening operations can yield significant benefits and impact overall productivity and profitability (Wills and Napier-Munn, 2006).

Continuous advancements in computer processing capacity have facilitated the adoption of more accurate simulation methods, such as the discrete element method (DEM). Over the years, DEM has become highly useful in representing realistic screening operations, helping to overcome the limitations of phenomenological and empirical models. DEM, first introduced by Cundall (1971) and further detailed by Cundall and Strack (1979), precisely represents dynamic processes such as segregation, passage, and transport, making it highly suited for the simulation of screening operations.

Recent studies have demonstrated the effectiveness of DEM in optimizing screening performance. For instance, Jiang et al. (2021) and Polanía et al. (2023) investigated the impact of particle shape and size on screening efficiency, revealing significant effects on the screening process. Similarly, Wang et al. (2023) and Liu et al. (2023) optimized vibration parameters like frequency, amplitude, and direction, showing enhancements in vibrating screen performance. Additionally, the optimization of banana screens using DEM has proven to improve unit-time screening efficiency (Extrica, 2023).

Earlier attempts at DEM modeling of screening, as described by Shimosaka et al. (2000), Li et al. (2002; 2003), Hilden (2007), Cleary et al. (2009a, 2009b), Dong and Brake (2009), Chen and Tong (2010), Zhao et al. (2011), Delaney et al. (2012), Elskamp

* Corresponding author: first.author@e-mail.address.com • https://orcid.org/0000-0000-0000-0000
** second.author@e-mail.address.com • https://orcid.org/0000-0000-0000-0000
*** third.author@e-mail.address.com • https://orcid.org/0000-0000-0000-0000

https://DOI: 10.30797/madencilik.1469819

and Kruggel-Emden (2015), Jahani et al. (2015), Zhao et al. (2017), Elskamp et al. (2017), Cleary et al. (2018), and Aghlmandi Harzanagh et al. (2018), explored various parameters using DEM. However, few studies have addressed the validation of created models (Hilden 2007; Delaney et al. 2012; Zhao et al. 2016; Aghlmandi Harzanagh et al. 2018).

After successful validation of the DEM model developed using a pilot-scale vibrating screen and studying the effects of some design and operational parameters (such as feed flow rate, vibration amplitude, screen deck inclination, vibration direction, and vibration frequency) in the previous study (Aghlmandi Harzanagh et al., 2018), this current study addresses the influence of screen surface parameters (i.e., screen surface dimensions, aperture shape, and surface open area) on the screening performance of a vibrating pilot-scale screen. This study focuses on surface parameters with a perspective meaningful for mineral processing experts and evaluates these parameters using classic evaluation approaches.

The researchers utilized the open-source LIGGGHTS software (Kloss et al., 2012) to conduct DEM simulations. Within these simulations, multi-spheres (sphere clumps) were employed to model irregularly shaped particles. The effects of various parameters on screening performance were investigated based on partition curve, cut-size, imperfection, screening efficiency, mean residence time of particles, and more.

1. Geometry and Simulation Setup of the Pilot-Scale Vibrating Screen

Similar to the validation of DEM simulations performed in the previous study (Aghlmandi Harzanagh et al. 2018), this study focuses on the investigation of additional screen surface parameters on a pilot-scale vibrating inclined screen. The present study employed the Hertz-Mindlin particle contact model, with a comprehensive description available in Jahani et al. (2015). For conducting DEM simulations, the researchers utilized the open-source LIGGGHTS solver. To facilitate the simulations, they prepared various 3D models of the screen. Fig. 1, shows the pilot scale vibrating screen and its CAD model alongside the available feeding system. The polyurethane screen surface is comprised of six square panels in length and two in width, resulting in overall dimension of 90×30cm. The screen surface was inclined at an angle of 10 degrees to facilitate the study. Table 1 provides the size distribution of the feed material and DEM model parameters that were used in DEM simulations. This table compiles the essential parameters and variables used as inputs in the simulations to accurately model the screening process.

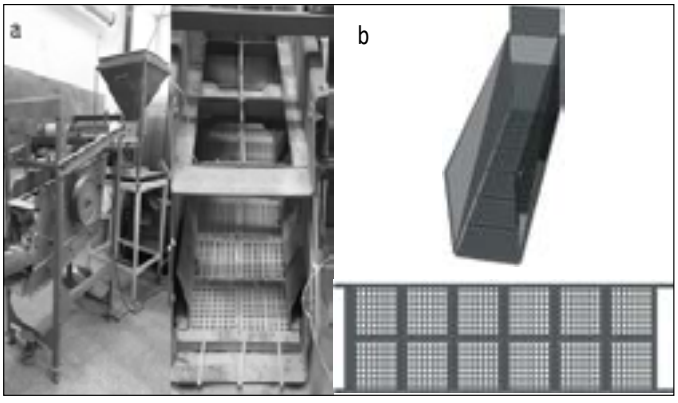

Fig. 1. (a) Real version of the vibrating screen and feeder system. (b) CAD version of the vibrating screen

Table 1. The data used in DEM simulations.

Feed size distribution	
Size (mm)	Weight (%)
26.6	10
20.6	10
15.7	20
12.1	8
9.5	14
6.7	14
4.7	14
2.8	10

Parameter	Value
Type of vibration	Linear oscillatory motion Amplitude: 4mm Frequency: 25Hz Direction: 95° according to horizontal axis
Particle density (kg/m^3)	2700
Modulus of elasticity (N/m^2)	5×10^7
Poisson's ratio	0.45
Restitution coefficient	0.3
Sliding friction coefficient	0.5
Rolling friction coefficient	0.01
Time Step (s)	5×10^{-6}
Simulation timeframe (s)	In the range of 25-35

The model parameters, such as Young's modulus (modulus of elasticity), time-step, Poisson's ratio, etc., were thoroughly tested through several simulations in alignment with previous studies in the literature. This rigorous testing aimed to ensure the accuracy and reliability of the DEM model in accurately representing the screening process. Multiple simulations were conducted to achieve a suitable time-step based on the concept of "Rayleigh time," ensuring practical and efficient simulation durations. This approach aimed to strike a balance between computational efficiency and maintaining accurate representation of the screening process.

Numerous simulations were performed at various screen surface dimensions, aperture shapes and open area values while holding all other parameters constant to examine how different parameters affect screening performance. Non-spherical particles were utilized in the simulations. While modelling irregular particle shapes, multi-spheres (sphere clumps) method of LIGGGHTS' multi-sphere module was used. This method uses sphere clumps for the creation of a new non-spherical particle. To implement this method, coordinates of the centers and radii of the spheres need to be imported into the solver through a text file. The simulation supports the utilization of several particle templates, providing the flexibility to incorporate diverse particle shapes and properties within a single study. To create a new non-spherical particle with an optimal number of spheres, the authors developed an in-house program which takes the CAD model of a high-resolution particle, reduces the number of vertices to the desired resolution, and then fills the volume with spheres. This innovative approach allows for efficient and accurate representation of particles in the DEM simulations while maintaining computational feasibility. Using this methodology, a sphere is created at each vertex and expanded until it touches any other vertex. After iterating this process for every vertex, a simplified sphere clump representation of the particle is obtained (Fig. 2). The resulting sphere clump serves as an efficient and effective model for the irregularly shaped particles in the DEM simulations. Table 2 shows the values of parameters used in the simulations.

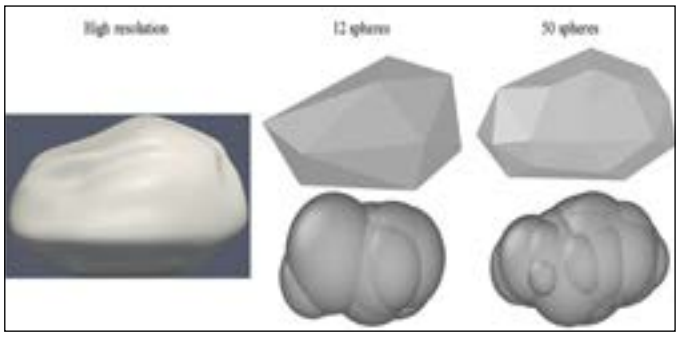

Fig. 2. The stages of creating a non-spherical particle template

Table 2. List of values of parameters used in simulations

Parameter	Values
Surface length (cm)	60, 75, 90
Aspect ratio of the aperture	2H*, 2V*, 3H, 3V, 4H, 4V
Surface open area	21.78, 16, 11.11

* relative to the horizontal / vertical

The simulation starts by creating and letting particles fall from the virtual feeder under gravity. As these particles reach and move along the screen surface, they either pass through the surface or flow along it towards the discharge, replicating real-world screening behavior in the DEM simulations. In order for a proper evaluation, the screen operation needs to achieve the steady-state (namely, the inlet flow rate equals the combined flow rates of the oversize and undersize streams for each size fraction). Therefore, the data in the first few seconds until the steady-state is maintained are disregarded. A typical illustration of the simulations is given in Fig. 3, which shows a visual representation of the particle motion during screening.

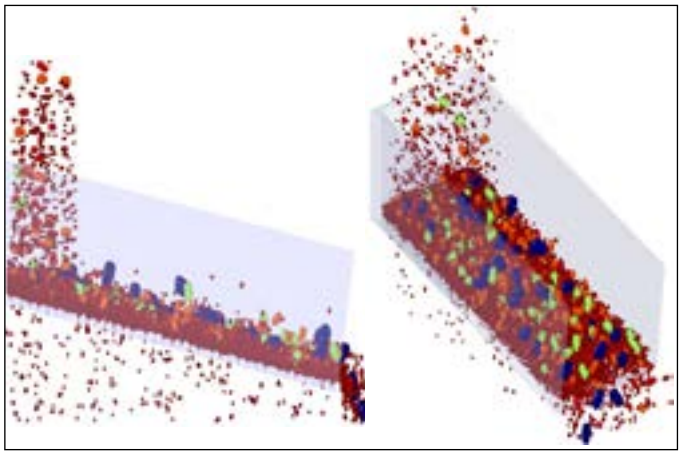

Fig. 3. Typical illustration of simulations

At the end of the simulations, the data files were obtained which includes the coordinates, velocity, acceleration and force of each particle at each time step. These data were then used to calculate the residence time of individual particles or particle size classes on the screen surface and to determine whether the screen has reached a steady state. These precise data points provide critical insights into the screening process and aid in analyzing the behavior and performance of particles throughout the simulation duration.

2. Results and Discussion

Depending on the simulation parameters, substantial amount of data is generated in each simulation which includes the location, velocity, angular velocity, and torque of each particle at every time step. This data can be visualized using suitable post-processing software to gain insights from the simulation results. OVITO (Open Visualization Tool) was used for the visualization of DEM data. Researchers designed and implemented an in-house program to extract essential information from the extensive dataset. This custom program was developed to efficiently process and analyze the simulation data, enabling the extraction of the required results. The custom program reads and analyzes the data files obtained in the simulations, extracts crucial information such as the system's state (steady or unsteady), final fractionation of particles to products (undersize or oversize stream), the size distributions of both (coarse and fine) products, as well as the residence time of each particle on screen.

Equation 1 was utilized to determine the overall screening efficiency (Wills and Napier-Munn, 2006).

$$E = \frac{c\text{-}f}{c(1-f)} E = \frac{c\text{-}f}{c(1-f)} \qquad \text{Equation 1}$$

The fractions f and c in Equation 1 correspond to the material within a size range in the feed and oversize streams, respectively. The study also involved calculating and plotting partition curves for each size fraction, representing the percentage of the feed reporting to the oversize product. This analysis provided valuable insights into the distribution of material across different size ranges during the screening process. Partition curves were then used to determine the separation size of the screen and the sharpness of separation which is an indication of the efficiency of separation. The efficiency and sharpness of the screening is a measure of the slope of the middle section of the partition curve. The inefficiency of separation, or the so-called imperfection, *I*, is then given by:

$$I = \frac{d_{75}\text{-}d_{25}}{2d_{50}} I = \frac{d_{75}\text{-}d_{25}}{2d_{50}} \qquad \text{Equation 2}$$

the sharpness and therefore efficiency of the screening decreases by increasing of the imperfection value (Wills and Napier-Munn, 2006).

Moreover, the study encompassed the calculation of mean residence times of particles for each size fraction, which served as an additional indicator of separation efficiency. This analysis provided valuable information about how long particles of different sizes remained within the system during the screening process, contributing to a better understanding of the overall performance. Discrete element modeling provides a unique opportunity to evaluate particle behavior under various conditions, including the reliable calculation of mean residence times for different size fractions. This capability is difficult to achieve through traditional experimental methods in actual screening operations.

2.1 Effects of screen surface dimension

The dimensions of the screen surface, especially the length of the screen (stream direction), affects the screening performance by controlling the particles' residence time and the bed depth, whereas the width of the screen determines the capacity of the screen. As the length of the screen increases, particles spend more time on the screen surface which increases the possibility of fine particles passing through the apertures. To examine these effects, three different screen surfaces with various lengths were designed. Designed screen surfaces have 4, 5 and 6 longitude panels, the dimension of each panel being 15×15cm (Fig. 4). During the simulations, 10.5mm square apertures were used.

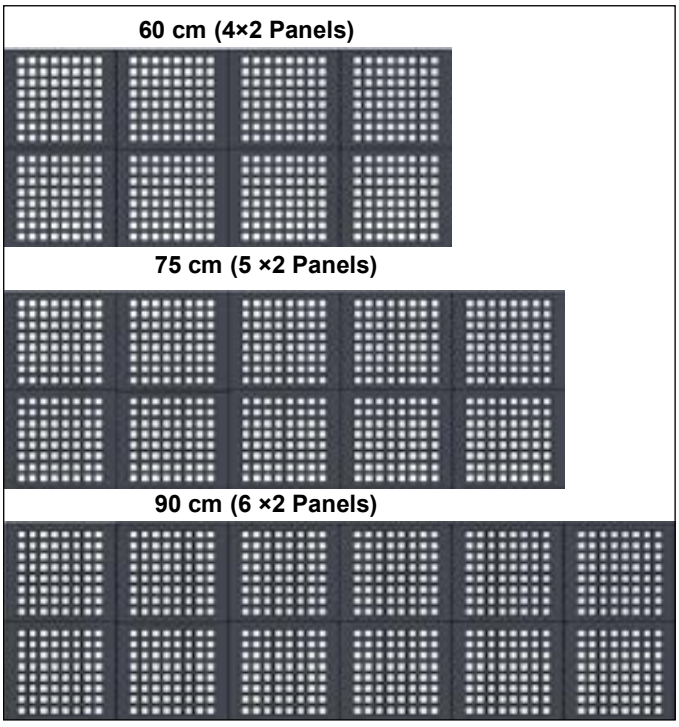

Fig. 4. Screen surfaces with different lengths

In order to be able to isolate the effects of the length of the screen surface, the other parameters like feed flowrate (25 t/h), feed size distribution, vibration parameters (amplitude, frequency and direction), etc. were kept constant in these simulations (Table 1).

As expected, the results of simulations show that the longer screen surface provides higher efficiency and higher mass recovery in the undersize stream (Fig. 5).

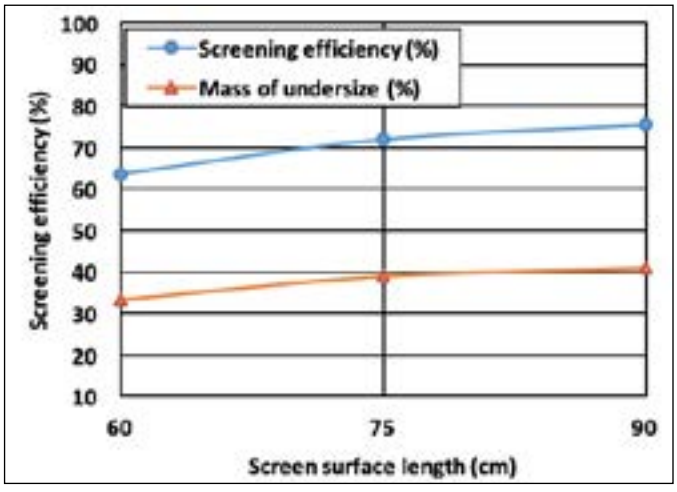

Fig. 5. Effects of length of screen surface on screening efficiency and mass of undersize stream

Fig. 6 shows the partition curves of the separation performed at various surface lengths. The d_{25}, d_{50}, d_{75} values and the calculated imperfections of the separations at different screen surfaces lengths are given in Table 3.

Partition curves and imperfection values indicate that longer sieves work more efficiently and also cut-size is higher in longer surfaces as expected. According to Fig. 6, the differences in the partition coefficients are more pronounced in finer particles (2.8, 4.7 and 6.7mm) rather than the near mesh particles (9.5mm) which shows that efficiency-oriented effects of surface length is observed as an improvement of the passing of fine particles.

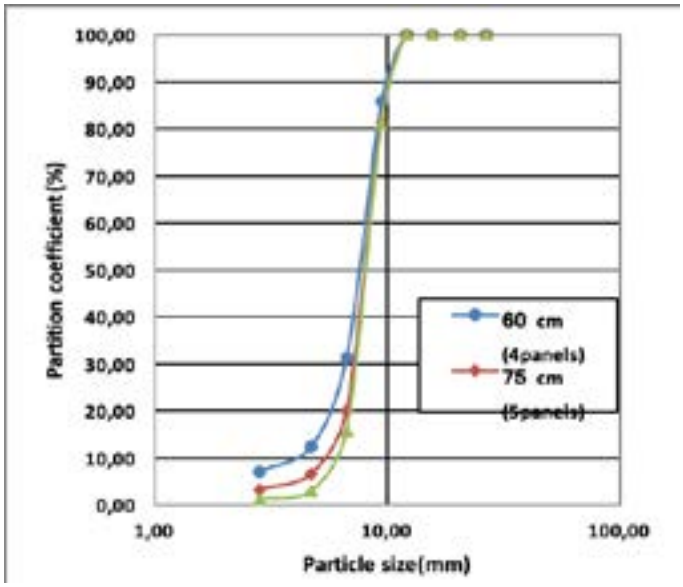

Fig. 6. Partition curves at different screen surface lengths

Table 3. Performance parameters for different screen surface lengths

Screen Length	d_{25}	d_{50}	d_{75}	Imperfection
60 cm	6.25	7.60	8.80	0.17
75 cm	6.95	8.00	9.10	0.13
90 cm	7.15	8.10	9.10	0.12

Fig. 7 illustrates the mean residence time (MRT) of particles reporting to oversize and undersize streams across different screen surface lengths. In the case of particles reporting to undersize stream, the MRT is increasing with increasing particle size in all cases which indicates that fine particles pass through apertures in the initial parts of the screen whereas larger particles pass mainly in the latter parts, spending more time on the screen surface and the bed. On the other hand, increasing the surface length causes an increase in the mean residence time of particles, however this increase is more pronounced for near mesh and middle-sized particles (9.5 and 6.7mm). The larger particles need more time to pass and longer screen surfaces provide extra time to these particles and therefore improve the overall screening efficiency.

In the case of particles reporting to oversize stream, the mean residence time of the finest particles is the minimum in all of the simulations, but MRT increase with increasing particle size and reaches a maximum value for near mesh particles and follows a decreasing trend with increasing particle size. This is an important observation because the time the particle spends on the screen surface would be an indication of the bed depth. The existence of fine particles (2.83 mm) in the oversize stream are due to their misplacement and not finding a chance to contact to screen surface. It is observed in the simulation animations that very fine and very coarse particles leave the screen surface placing in top layers of material bed with minimum interaction with screen surface but other particles with sizes towards near mesh size (9.5mm) locate in lower positions of the material bed and therefore have higher interaction with screen surface. This finding agrees well with the mean residence time of particles reporting to oversize stream (Fig. 7)

As can be seen in Fig. 7, increasing in surface length causes an upward shift in MRT curves as higher lengths mean larger residence times on the screen surface.

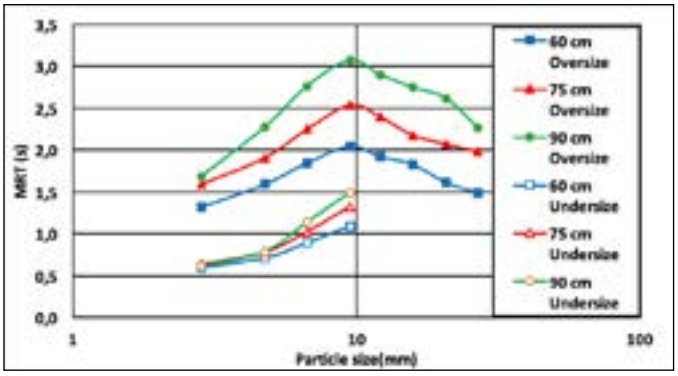

Fig. 7. Mean residence time of particles at various screen surface lengths

2.2 Effects of aperture shapes

It is well-known that in the screens with rectangular apertures, the flow-oriented apertures serve the purpose of capacity while apertures perpendicular to the flow direction are useful to maintain high screening efficiencies (Dong et al. 2016). In order to have a deep insight on how aperture orientation affects the screening process, six different screen surfaces with various aperture aspect ratios and orientations were designed. Simulations were performed using these 3D models keeping other parameters constant (Table 1). Fig. 8, shows the single panel of each designed screen surface. Complete screen surface models consist of 12 panels (2×6).

As per the simulation results, the screening efficiency demonstrated an upward trend with an increase in the aspect ratio of the aperture. Additionally, at the same aspect ratio, the screen with apertures perpendicular to the flow direction have higher screening efficiency in the case of screen surfaces with rectangular apertures (Fig. 9).

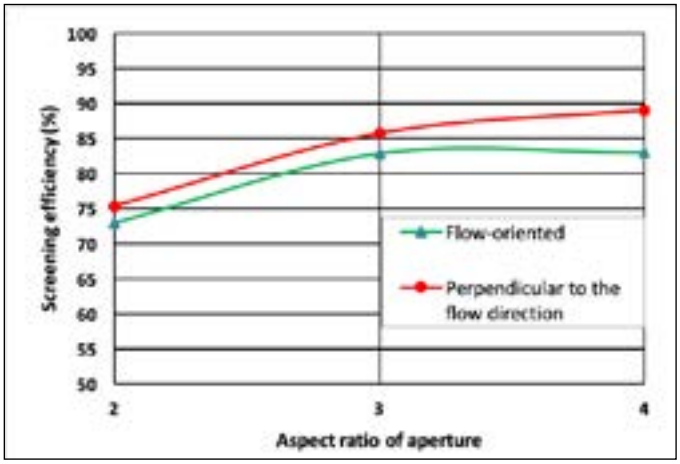

Fig. 9. Effects of aspect ratio and orientation of the screen aperture on the screening efficiency

Fig. 10, shows the respective partition curves for the simulations performed at various aperture aspect ratios and orientations and Table 4 shows the Imperfection values for performed simulations. According to Fig. 10 and Table 4, at constant aspect ratio, generally the partition curves of screening processes performed by screen

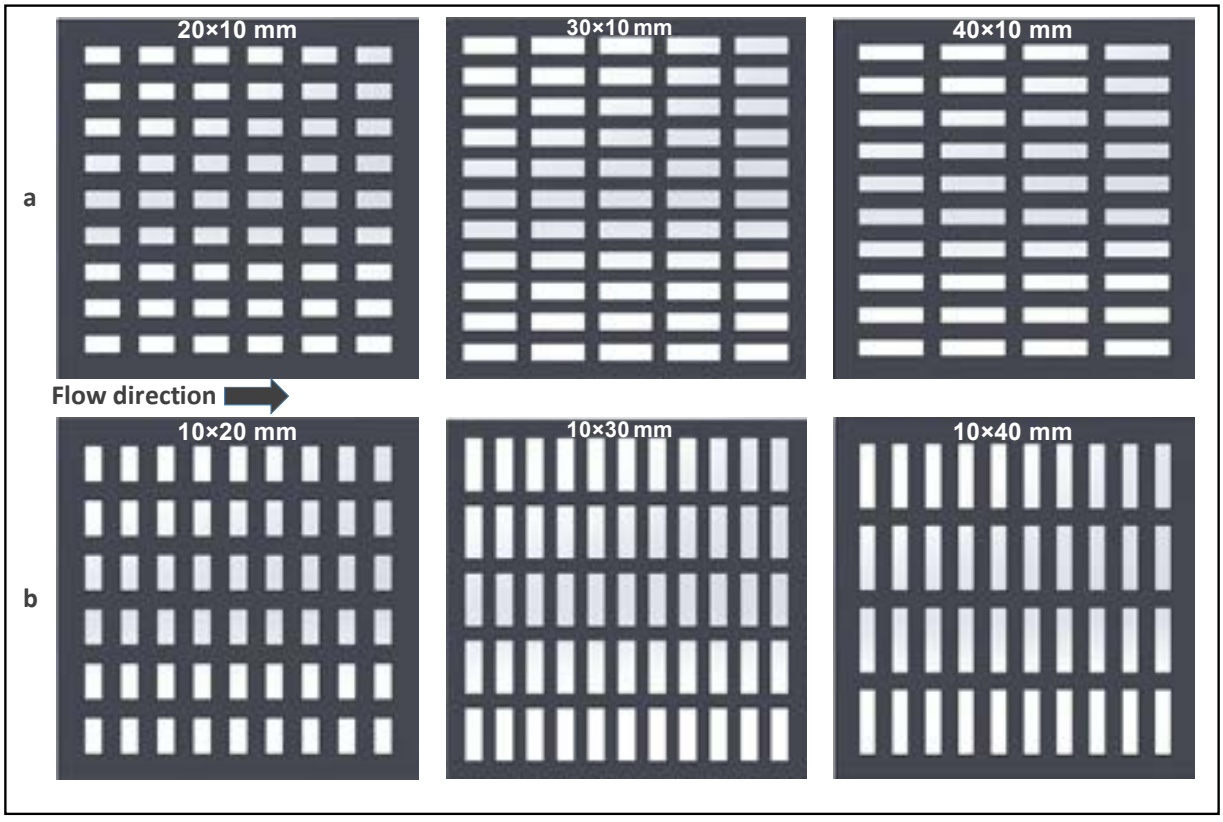

Fig. 8. Schematic view of designed screen surfaces with apertures at various aspect ratio and orientation (a: flow-oriented apertures, b: perpendicular to the flow direction apertures)

apertures perpendicular to the flow direction are a bit sharper (smaller Imperfection values) and the partition coefficient of near mesh particles (9.7mm) are smaller which shows that the screening is much more efficient. The results show that, regardless of the orientation of apertures, the sharpness of partition curves increases with increasing aspect ratio of screen aperture which means that an increase in aspect ratio of rectangular apertures increases the efficiency of the screening process.

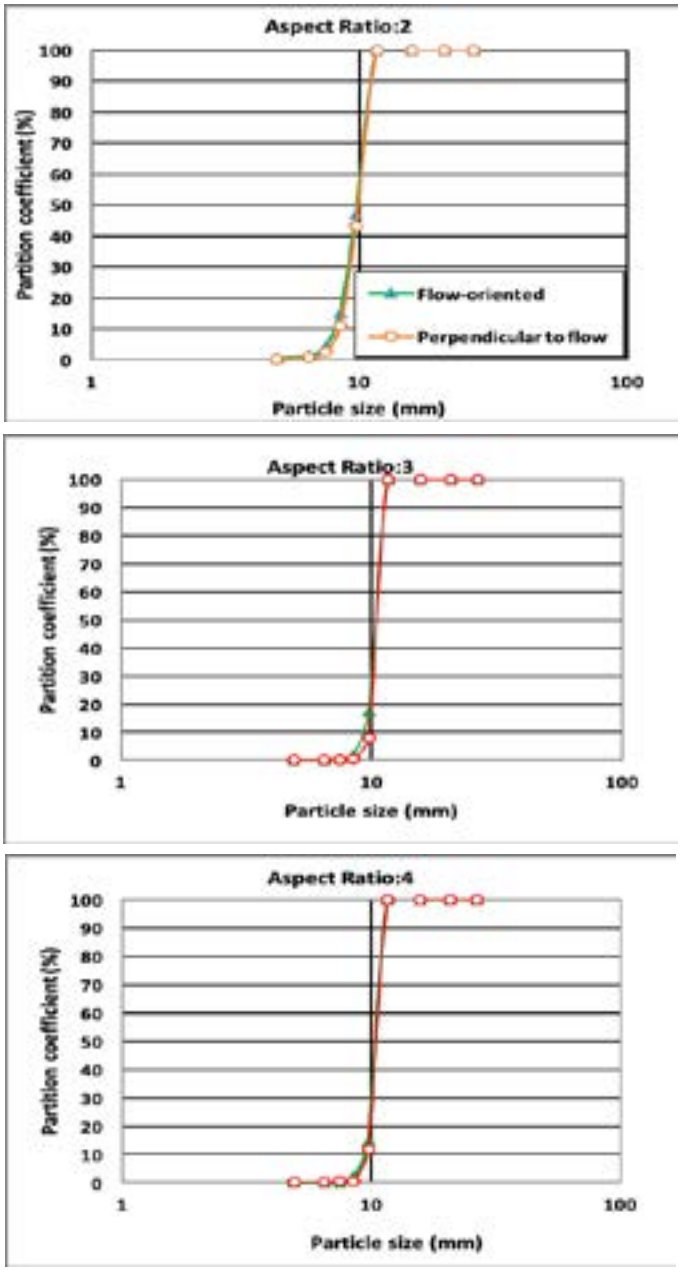

Fig. 10. Partition curves at various aperture aspect ratios and orientations

The investigation of mean residence time (MRT) for particles reporting to undersize and oversize streams with various aperture shapes (Fig. 11) reveals that MRT is higher for both particle types (oversize and undersize) across all particle sizes when using screens with apertures perpendicular to the flow direction. Although perpendicular orientation provides particles more time on screen surface and increases the probability of passing through apertures resulting in higher efficiency, higher residence time causes the accumulation of more particles on the screen surface and eventually resulting in lower screening capacity. Table 4. Imperfection values for different aspect ratios and orientations of screen apertures

Table 4. Imperfection values for different aspect ratios and orientations of screen apertures

Aspect Ratio	Direction	d_{25}	d_{50}	d_{75}	Imperfection
2	flow-oriented	8.90	9.85	10.50	0.081
	perpendicular to the flow	9.10	9.90	10.60	0.076
3	flow-oriented	9.90	10.40	10.90	0.048
	perpendicular to the flow	10.03	10.43	10.95	0.044
4	flow-oriented	10.00	10.45	10.90	0.043
	perpendicular to the flow	10.05	10.50	10.90	0.040

Fig. 12, shows the displays of screens and particles at 20th second of the performed simulations. The relative increase in bed depth and particle accumulation at the screen surface is observable in simulations performed by screens with perpendicular to the flow-oriented apertures (right column).

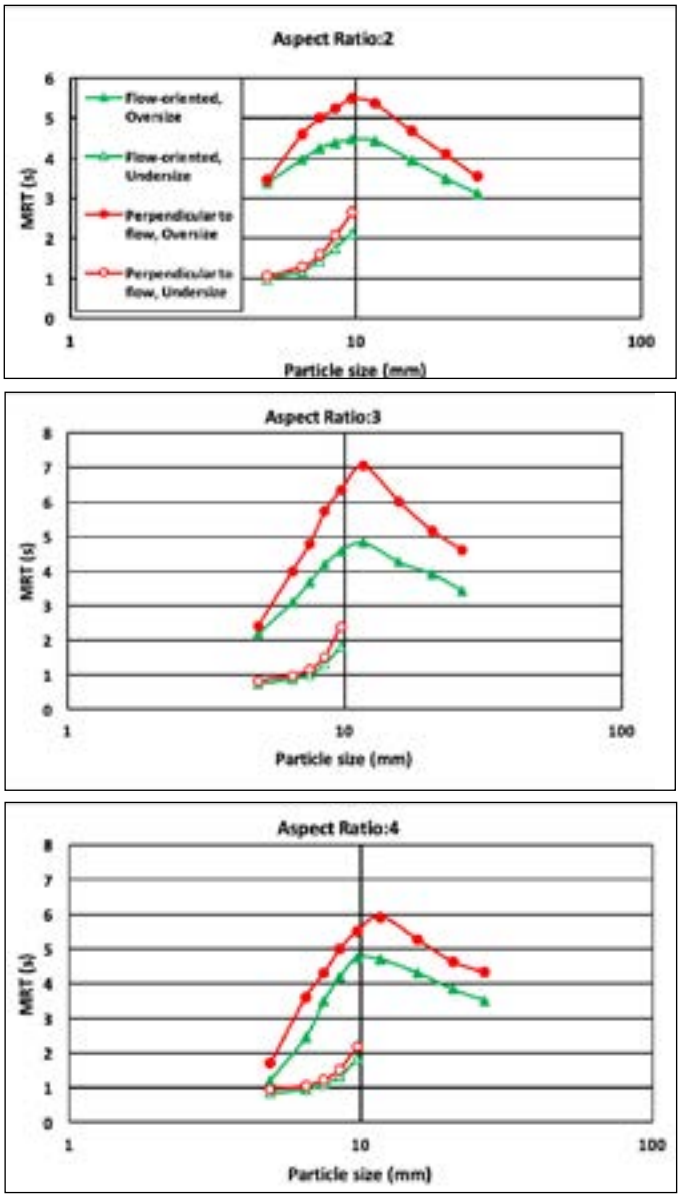

Fig. 11. The mean residence time of the particles reported to undersize and oversize streams at various aperture aspect ratios and orientations

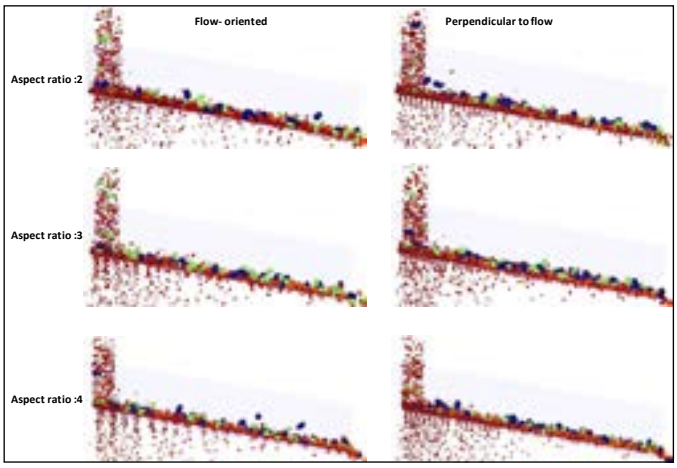

Fig. 12. The steady-state views of screens and particles obtained from the simulations performed at various aperture types

2.3 Effects of screen surface open area

The ratio of the total area of the openings in the screen surface to the total area of the screen surface is expressed as open area. It is well known that increasing the open area improves the screening efficiency by increasing the number of apertures. To examine the effects of open area on screening performance and particle behaviors, three different screen surfaces were designed. The surface dimensions (900×300mm) and aperture sizes (10×10mm) were kept constant in 3D models but the spaces between apertures were considered as 10, 14 and 20mm (Fig. 13). The open areas of these 3D models were calculated as 21.78, 16.00 and 11.11% respectively. The screen surface was constructed as 2x6 panels.

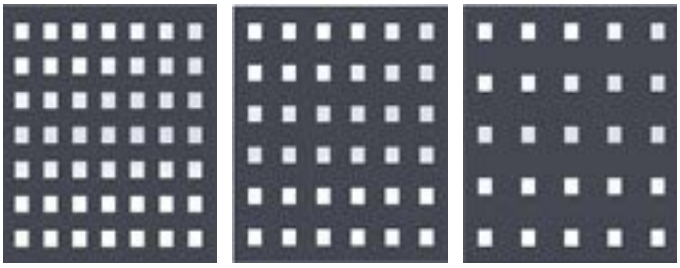

Fig. 13. Schematic view of screen surface 3D models with different screen surface open areas (single panel)

For isolating the effects of surface open area, other design and operating parameters like feed flowrate (25t/h), size distribution of the feed, vibration properties, surface inclination and etc. were kept constant in simulations (Table 1).

According to the results of the simulations, as expected, screening efficiency and mass of undersize increases by increasing surface open area (Fig. 14). The study of respective partition curves (Fig.table 15) together with d_{25}, d_{50}, d_{75} and the imperfection values (Table 5) exposes significant differences in both separation sharpness and cut-point-size as higher open areas offer steeper sharpness and higher cut-point-size. Calculated cut-point-sizes for screening at open area values of 21.78, 16.00 and 11.11% are 6.62, 5.93 and 5.18 mm respectively. it is apparent from partition curves that, despite the small difference between partition coefficients at near mesh particles (8.4mm), this gap is more pronounced for finer particles (2.8, 4.9, 6.4 and 7.4mm) which means that increasing the open area of the screen surface improves the screening efficiency mostly by increasing the recovery of the finer particles to undersize stream.

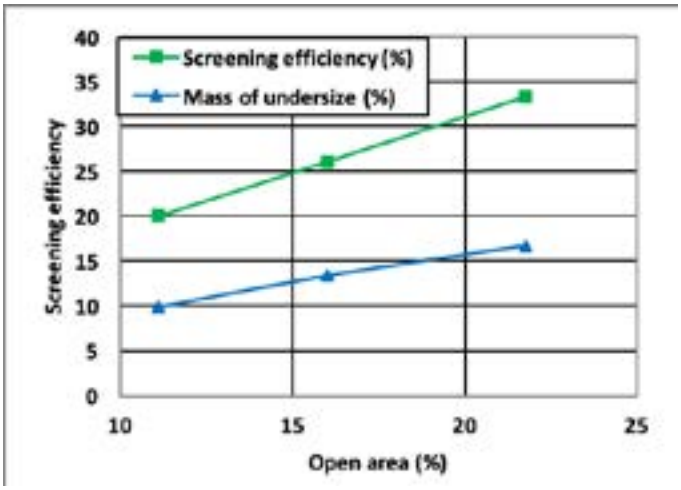

Fig. 14. Effects of the surface open area on screening efficiency and mass of undersize stream.

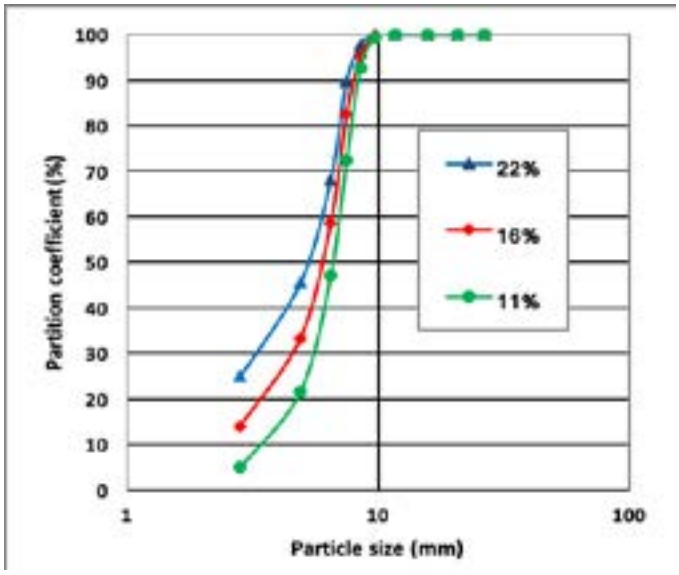

Fig. 15. Partition curves at various levels of surface open area

Table 5. Imperfection values for different screen surface open areas based on partition curves

Open Area (%)	d_{25}	d_{50}	d_{75}	Imperfection
11.11	2.83	5.18	6.83	0.39
16.00	4.00	5.93	7.15	0.27
21.78	5.20	6.62	7.60	0.18

Fig. 16, shows the mean residence time of the particles reporting to undersize and oversize streams at various surface open area values. Apparently, the mean residence time of both undersize and oversize particles on screen surface is higher in screen surfaces with larger open area. Larger open area means higher number of apertures on the surface causing more interaction between particles and screen surface which increase the MRT and particle accumulation on the screen surface. Although accumulation of particles looks like a negative effect on screening, under the influence of vibration and formation of a dynamic bed material on screen surface usually results in superior screening performance by segregation and placing fine and near mesh particles closer to the screen surface.

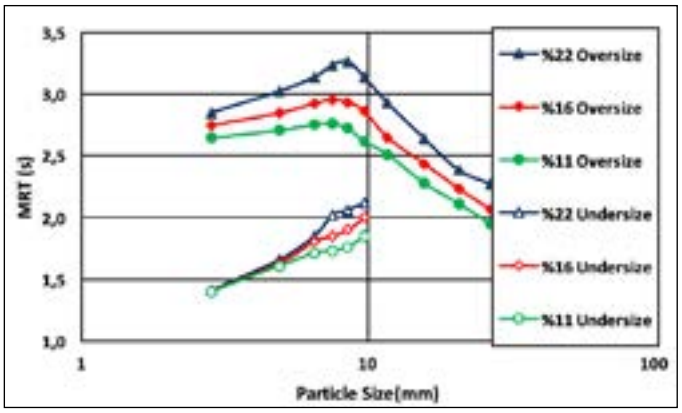

Fig. 16. The mean residence time of particles reporting to undersize and oversize streams at various surface open areas

3. conclusions

n this study, a three-dimensional DEM model was employed to numerically simulate the particle flow in a typical pilot-scale vibrating screen. The simulations utilized non-spherical particles, allowing for a more accurate representation of the real-world screening behavior. The effects of parameters related to the screen surface, such as surface dimensions, aperture shape and surface open area, on screening performance were investigated. The performance of the screening was evaluated in terms of screening efficiency, mass flow of the undersize stream, partition curves, imperfection values, cut-size, and mean residence time of the particles.

Key findings include:

- Longer screen surfaces increased screening efficiency and mass recovery in the undersize stream.
- Screens with perpendicular apertures to the flow direction achieved higher screening efficiency compared to those with flow-oriented apertures.
- Increased surface open area improved screening efficiency by enhancing the recovery of finer particles.

Acknowledgement

The authors express their sincere gratitude for the financial support provided by The Scientific and Technological Research Council of Turkey (TUBITAK) for the project titled "Numerical Modelling of Industrial Screening" (215M368).

References

Aghlmandi Harzanagh, A., Orhan, E.C., Ergun, S.L., 2018. Discrete element modelling of vibrating screens. Miner. Eng. 121, 107–121. doi:10.1016/j.mineng.2018.03.010

Beas, I.N., & Nongwe, I. (2021). An Overview of Plastic Waste Generation and Management in Food Packaging Industries. Recycling, 6(1), 12. https://doi.org/10.3390/recycling6010012

Chen, Y., Tong, X., 2010. Modeling screening efficiency with vibrational parameters based on DEM 3D simulation. Min. Sci. Technol. 20, 615–620. doi:10.1016/S1674-5264(09)60254-4

Cleary, P.W., Sinnott, M.D., Morrison, R.D., 2009a. Separation performance of double deck banana screens – Part 1: Flow and separation for different accelerations. Miner. Eng. 22, 1218–1229. doi:10.1016/j.mineng.2009.07.002

Cleary, P.W., Sinnott, M.D., Morrison, R.D., 2009b. Separation performance of double deck banana screens – Part 2: Quantitative predictions. Miner. Eng. 22, 1230–1244. doi:10.1016/j.mineng.2009.07.001

Cundall, P.A., 1971. A computer model for simulating progressive large-scale movements in blocky rock systems. Nancy, p. Symp. Int. Soc. Rock Mech.

Cundall, P.A., Strack, O.D.L., 1979. A discrete numerical model for granular assemblies. Géotechnique 29, 47–65. doi:10.1680/geot.1979.29.1.47

Delaney, G.W., Cleary, P.W., Hilden, M., Morrison, R.D., 2012. Testing the validity of the spherical DEM model in simulating real granular screening processes. Chem. Eng. Sci. 68, 215–226. doi:10.1016/j.ces.2011.09.029

Dong, K., Esfandiary, A.H., Yu, A.B., 2016. Discrete particle simulation of particle flow and separation on a vibrating screen: Effect of aperture shape. doi:10.1016/j.powtec.2016.11.004

Dong, K.J., Brake, I., 2009. DEM simulation of particle flow on a multi-deck banana screen. Miner. Eng. 22, 910–920. doi:10.1016/j.mineng.2009.03.021

Elskamp, F., Kruggel-Emden, H., 2015. Review and benchmarking of process models for batch screening based on discrete element simulations. Adv. Powder Technol. 26, 679–697. doi:10.1016/j.apt.2014.11.001

Elskamp, F., Kruggel-Emden, H., Hennig, M., Teipel, U., 2017. A strategy to determine DEM parameters for spherical and non-spherical particles. Granul. Matter 19, 46. doi:10.1007/s10035-017-0710-0

Extrica. (2023). Performance optimization of banana vibrating screens based on PSO-SVR under DEM simulations. Retrieved from https://www.extrica.com

Hilden, M.M., 2007. Dimensional analysis approach to the scale-up and modelling of industrial screens. PhD-thesis, University of Queensland.

Jahani, M., Farzanegan, A., Noaparast, M., 2015. Investigation of screening performance of banana screens using LIGGGHTS DEM solver. Powder Technol. 283, 32–47. doi:10.1016/j.powtec.2015.05.016

Jeanger, P.J., Labayen, I.V., & Yuan, Q. (2022). A Review on Textile Recycling Practices and Challenges. Textiles, 2(1), 174-188. https://doi.org/10.3390/textiles2010010

Jiang, Z., Zhang, C., & Zhao, Y. (2021). Quantification of the contribution ratio of relevant input parameters in DEM-based granular flow simulation. Powder Technology, 383, 313-322. https://doi.org/10.1016/j.powtec.2021.01.075

Kloss, C., Goniva, C., Hger, A., Amberger, S., Pirker, S., 2012. Models, algorithms and validation for open-source DEM and CFD-DEM. Prog. Comput. Fluid Dyn. 12, 140–152.

Li, J., Webb, C., Pandiella, S.S., Campbell, G.M., 2002. A Numerical Simulation of Separation of Crop Seeds by Screening—Effect of Particle Bed Depth. Food Bioprod. Process. 80, 109–117. doi:10.1205/09603080252938744

Liu, Q., Tang, S., & Zhang, X. (2023). A coupled FEM-DEM study on mechanical behaviors of granular soils considering particle breakage. Computers and Geotechnics, 143, 104551. https://doi.org/10.1016/j.compgeo.2021.104551

Polanía, A.F., Awich, J.V., & McCarthy, J.J. (2023). DEM study on the role of fines in the mobility of dry granular flows. Powder Technology, 391, 482-492. https://doi.org/10.1016/j.powtec.2021.01.076

Shimosaka, A., Higashihara, S., Hidaka, J., 2000. Estimation of the sieving rate of powders using computer simulation. Adv. Powder Technol. 11, 487–502. doi:10.1163/156855200750172088

Wang, Z., Li, Y., & Liu, G. (2023). DEM-based parameter optimization and tests of digging green onions. International Journal of Agricultural and Biological Engineering, 16(2), 140-148. https://doi.org/10.25165/j.ijabe.20231602.6842

Wills, B.A., Napier-Munn, T.J., 2006. Mineral Processing Technology. Elsevier Science & Technology Books.

Zhao, L., Zhao, Y., Bao, C., Hou, Q., Yu, A., 2017. Optimisation of a circularly vibrating screen based on DEM simulation and Taguchi orthogonal experimental design. Powder Technol. 310, 307–317. doi:10.1016/j.powtec.2017.01.049

Zhao, L., Zhao, Y., Bao, C., Hou, Q., Yu, A., 2016. Laboratory-scale validation of a DEM model of screening processes with circular vibration. Powder Technol. 303, 269–277. doi:10.1016/j.powtec.2016.09.034

Zhao, L., Zhao, Y., Liu, C., Li, J., Dong, H., 2011. Simulation of the screening process on a circularly vibrating screen using 3D-DEM. Min. Sci. Technol. 21, 677–680. doi:10.1016/j.mstc.2011.03.010